ELECTROLYSIS-DRIVEN REVERSIBLE ACTUATION USING MICROMACHINED PH-SENSITIVE HYDROGEL

R. Campbell[1], D. Buton[1], S. H. Song[2], and A. Kim[1]
[1]Temple University, Philadelphia, USA
[2]Sook Myung Women's University, South Korea

ABSTRACT

While volume changing hydrogel is well studied for a sensing application, its mechanical actuation can also be implemented for a reversible actuation. In this paper, we present an electrolytically controllable soft actuator that utilizes a chemo-mechanical volume changing property of hydrogel. By incorporating micropatterning and electrolysis electrodes on a hydrogel surface, environmental stimuli (i.e., pH) can be localized, resulting in a precisely controlled, large displacement, reversible actuation. Patterned and non-patterned pH-sensitive poly(methacrylic acid-co-acrylamide) hydrogel is studied using a DC voltage (5 V). The hydrogel with a dimension of 5 mm by 5 mm by 0.5 mm with line patterns (t = 40 µm) via a laser machining demonstrated 2 mm in maximum actuation displacement, which is a three-fold improvement in the range of motion compared to a non-patterned hydrogel. It is anticipated that the presented actuator design and mechanism can be applied to an underwater walker or gripper.

KEYWORDS

Actuator, electrolysis, hydrogel, micromachining

INTRODUCTION

Soft actuators or soft robotics are a subfield of robotics that uses highly compliant materials, such as silicone, mimicking those found in a living organism. Due to this compliance, flexibility, and adaptability, soft robotics has caused considerable interest in the robotics community. Compared to its counterparts, soft actuators boast a broad array of mechanical actuation capabilities from simple material deformations to complex bending or twisting. The principle of such actuation utilizes various modalities, including pneumatic [1], shape-memory alloy [2], and magnetic [3]. When it is coupled with the microelectromechanical systems (MEMS), the resulting combination of properties is ideal for creating novel biomedical and environmental applications [4]. However, such soft robotics could move only submillimeter range due to a limitation in actuation modalities. Magnetic force mediated actuation has been one of the popular modalities for controlled motion at the milli- and micrometer scales for the past two decades [5]. However, its reliability has been demonstrated only at a short distance. Other modalities, such as thermal, electrical, or piezoelectric properties, are also available; however, most actuators require high voltage and several structural layers. Altogether, MEMS-based actuators have complicated fabrication processes [6].

In this paper, we present hydrogel-based soft robotics that actuates the out-of-plane manner by low-voltage mediated electrolysis. The actuation principle is based on the unique property of hydrogel that presents a reversible volume phase response to a pH stimulus. The surface of the hydrogel is engineered to include electrolysis electrodes and microgroove patterns. By applying DC voltage across the electrodes, electrolysis occurs on the surface of hydrogel, inducing localized pH change and thus swelling near the cathode and shrinking near the anode.

OPERATION PRINCIPLE

Electrolysis of water is a process widely used in industry, biology, and medicine; by applying direct current (DC) through a substance, a controlled chemical change is induced [7]. The electrolysis of water produces hydrogen and oxygen gases by the following reactions.

$$\text{anode:} \quad 2H_2O \leftrightarrow O_2(g) + 4H^+(aq) + 4e^-$$
$$\text{cathode:} \quad 4H^+(aq) + 4e^- \leftrightarrow 2H_2(g)$$
$$\text{net:} \quad 2H_2O(l) \leftrightarrow O_2(g) + 2H_2(g)$$

Since this reaction generates gases from liquid, this direct conversion of electrical energy to pressure-volume change has been utilized as the basis for various actuator applications, including dispensing systems, dosing systems, switches, microvalves. For example, Lee et al. reported the fabrication of electrolysis-driven microvalve for microfluidics [8]. However, this actuation scheme requires entrapment of the produced gas in a chamber.

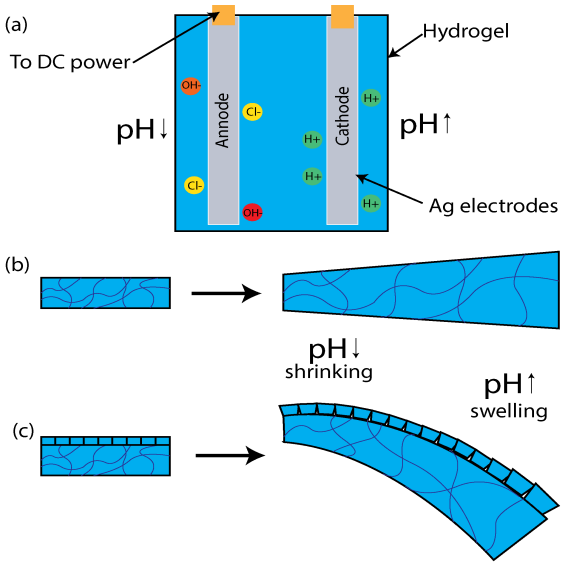

Figure 1: Electrolysis driven actuation of hydrogel: surface pattern (bottom right) enhances the actuation.

Another reaction result due to electrolysis would be the localized pH changes due to hydrogel at the cathode (increasing pH; alkalic) and hydroxy group (OH^-) at the anode (decreasing pH; acidic) as seen in Figure 1(a). Such electrolysis-driven pH change can be utilized for poly(mAA-co-AAm) hydrogel, whose swelling/shrinking

behaviors are well studied in our previous investigation [9], [10]. Hydrogel, a type of crosslinked polymer network, naturally absorbs a large amount of fluid. When the fluid carries a variety of chemical stimuli such as pH ion, antigens, temperature, or glucose, hydrogels mediates by the ionization of the functional groups. In our poly(mAA-co-AAm) hydrogel, phenylboronic acid (PBA) moieties exhibit gradual osmotic swelling forces in response to the pH [11]. When such hydrogel is stimulated by a pair of surface integrated electrodes and small DC voltage (~ 5V), via electrolysis, the anode side shrinks, and the cathode side swells due to two localized pH changes. The resultant behavior of the hydrogel, however, is not sufficient to be called actuation as its shape became a trapezoid. However, changing the surface tension by adding slits is sufficient to induce actuation, as seen in Figure 1(b). As such, the hydrogel is featured with micro-patterning to facilitate a greater range of motion, as shown in Figure 1(c).

DESIGN AND FABRICATION

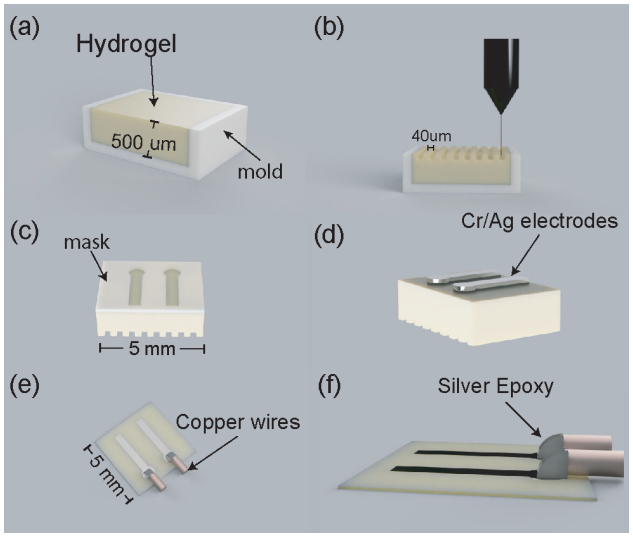

Figure 2: Actuator fabrication process: (a) hydrogel is cast in a mold, then (b) patterned with the laser machine. (c) a mask is applied and (d) electrode is evaporated on, (e-f) wires are attached using epoxy

The fabrication process for the electrolytic hydrogel actuator involved hydrogel preparation and device assembly. This provides a streamlined process for creating our actuator. Hydrogel preparation was based on our previous works [9], [10]. The pre-gel solutions for hydrogel were prepared. Part A is prepared by dissolving 277 mg of acrylamide, 84 µl of methacrylic acid, 83 µl of N,N,N′,N′ -tetramethylethylenediamine accelerator and 13.6 mg of N,N'-methylenebisacrylamide (cross-linker) into 1 ml of DI water and part B was prepared by adding 80 mg/ml ammonium persulfate to DI water. Then, part A and part B solution were mixed in a 5.9:1 ratio, respectively. The mixture was then synthesized to a thin film in polyester (PET) film mold ($5 \times 5 \times 0.5$ mm^3), Figure 2(a). After casting the hydrogel thin film, it was placed in a laser machine (Universal Laser Systems), where micro-grooves were ablated (40 µm apart). As the micro-grooves dictate the actuation direction, we patterned it as a line, Figure 2(b). The hydrogel is then completely dehydrated at room temperature for 24 hr. To prevent wrinkles during the dehydration, the hydrogel was laminated between PET with a small weight on top (100 g). Keeping the hydrogel dehydrated and wrinkle-free allowed the metal to adhere better during metal deposition. Using a shadow masking technique [12] that would avoid deterioration of hydrogel during metal deposition, Figure 2(c), the electrodes (Cr/Ag, 20/200 nm) were substantially deposited on the opposite side of the patterned surface (Eco-Vap, MBraun), Figure 2(d). Lastly, wires were attached to electrodes using silver epoxy, Figure 2(e-f). Figure 3 shows a picture of a final prototype. The resulting thickness of the actuator was 400 µm.

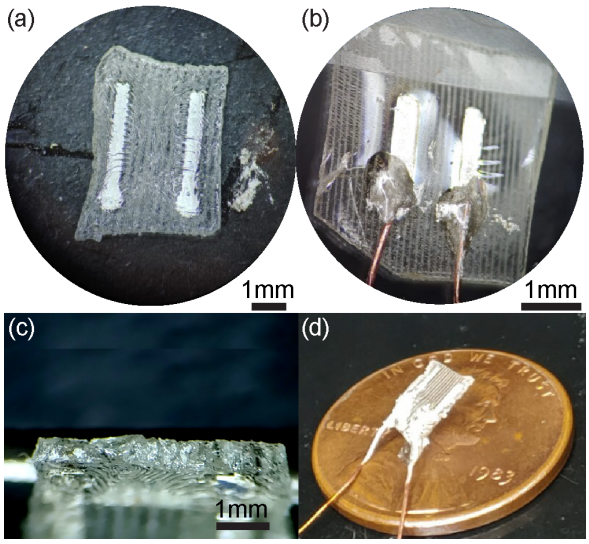

Figure 3: Fabricated prototype: (a) electrode on hydrogel, (b) with wires. (c) cross-sectional view, and (d) on a US penny

EXPERIMENTAL RESULTS

The soft hydrogel actuators were placed on a flat surface platform for testing. The actuation motion of each sample was video recorded and analyzed by each frame (60 fps). To study the effect of micro-groove, a hydrogel actuator without patterning was also prepared. Because the hydrogel was completely dried after the fabrication, it was required to rehydrate prior to the experiment. For this procedure, we applied fine mist using a humidifier for 10 min. Note that a droplet of water or submerging hydrogel in water may cause rapid water absorption, which could lead to uncontrolled actuation and electrode degradation. After the rehydration, a droplet of pH-indicator dye (phenolphthalein) was carefully applied to a wire-hydrogel junction to visually confirm the pH change during the electrolysis reaction. Lastly, all actuators were positioned at the same initial position along the edge of the platform. The DC voltage (5V) was applied across the electrodes for 10 min, then removed to determine if the actuator could return to its original shape. As electrolysis was initiated, we observed a pink color change in the phenolphthalein around the cathode (basic) and a yellow around the anode (acidic). This color change grew more visible with time and showed the pH change becoming more drastic. This color change was also used to assess the durability of the electrodes; the

electrode degradation due to electrolysis was identified by the visible outline of the affected areas, which were minor during the testing.

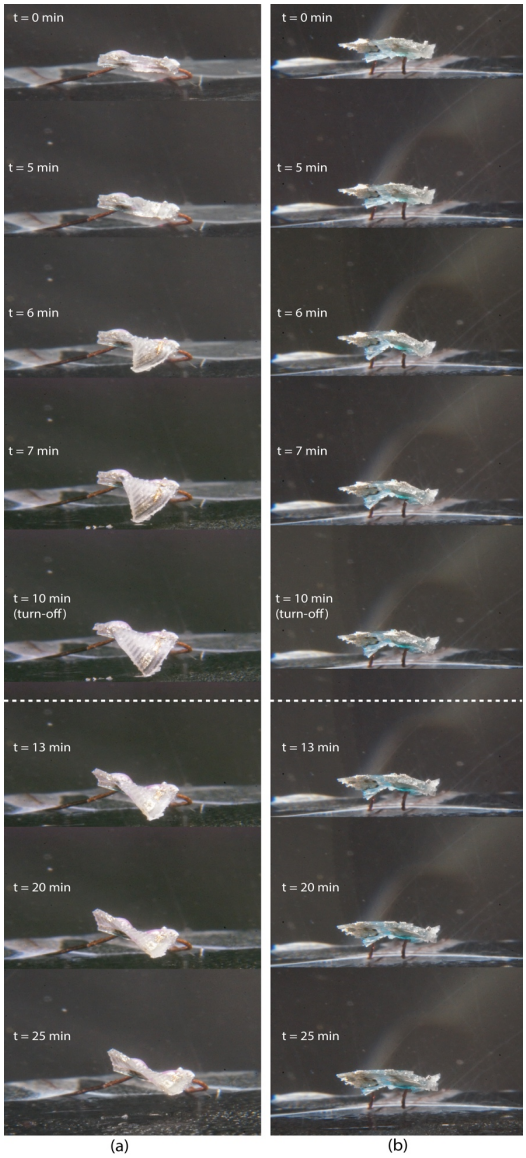

Figure 4: Key picture frames traced during actuation: (a) hydrogel actuator with micropattern, (b) hydrogel actuator without pattern. Scale bar represent 1 mm

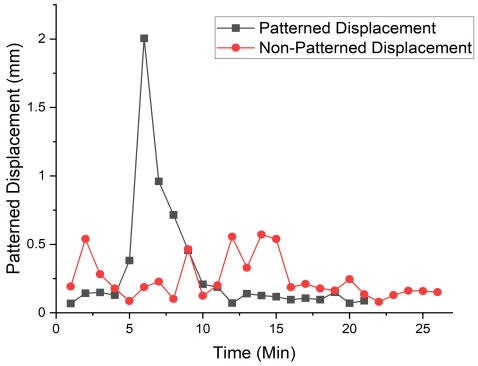

Figure 5: Displacement vs. time: hydrogel with micropattern exhibited the maximum displacement of 2 mm (Black), whereas non-patterned hydrogel (red) showed the maximum displacement of 0.6 mm comparison between points at each minute.

Figure 4 shows time-lapse pictures of hydrogel during electrolysis for 10 min and another 15 min after electrolysis is off. This process was done to both the case of the patterned, Figure 4(a), and non-patterned hydrogel, Figure 4(b). Overall, both hydrogel actuators exhibited asymmetric shapes (i.e., trapezoid) after electrolysis. The average measured thickness near cathode (pH > 8) was 480 µm (swelling behavior), and anode (pH < 5) was 310 µm (shrinking behavior). Therefore, the resulting actuation was twisting and folding motions with the cathode being the axis of rotation. The speed of actuation was 0.02 mm/s. Both actuators show a maximum vertical displacement between 2 mm and 2.5 mm. At the cathode side (thickness = 480 µm during actuation), a ratio of displacement to thickness was measured to be 4.17. As seen in Figure 6, the addition of the micropatterns indeed improved the actuation significantly (330% improvement compared to non-patterned hydrogel). The captured images were point tracked on the cathode corner to characterize the actuation of the hydrogel. Figure 5 shows the maximum displacement of the patterned hydrogel, which was 2 mm. The non-patterned hydrogel actuated by 0.6 mm displacement.

Figure 6a shows the temporal displacements of the cathode corner of the micropatterned actuator. Subsets show the picture of the actuator with guidelines at its initial, final, and maximum displacement positions. Positions shown in green were when electrolysis was active, and ones in a red mark that electrolysis is inactive. Figure 6b shows the temporal displacement for the non-micropatterned actuator using the same conventions. The results show that both pattern and non-pattern hydrogel had similar trends of curving downward and then returning near its starting location. However, the micropatterned hydrogel shows a more controlled negative trend, whereas the non-micropatterned actuator showed both positive and negative displacement from its initial position. Although patterned hydrogel showed better actuation, non-patterned hydrogel had better hysteresis (Δd = 1.358 mm for patterned and 0.697 mm for non-patterned).

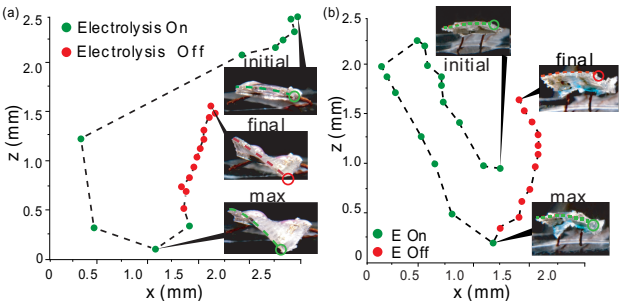

Figure 6: Cathode points tracking seen at XZ plane: (a) micropatterned hydrogel actuator and (b) non-patterned hydrogel actuator green dots indicate when electrolysis was applied, and red dots are when electrolysis was removed. Subsets display the actuators at its initial, max, and final position.

CONCLUSIONS

The hydrogel-based actuator exhibits promising results, making it a feasible candidate in future robotic and biomedical applications. The characterization verifies that

the actuator executes movement under electrolysis while maintaining low-cost, flexible, and pH-sensitive hydrogel discussed previously as indispensable elements of the actuator. Although it only displays a simple one-way curve, using different metal patterns can manipulate the hydrogel to implement more dynamic motions. With the addition of the micro-patterning, we can show a further range of motion. As we pair more intricate patterning with varying electrode shapes, we can expect the dynamic motion to increase further. This design also allows for modular expansion, where we can design different sections to do simple tasks in order to perform more complex motions. This will allow our system to perform precision tasks when working together. Optimization of the depth and spacing of the micropatterning will improve the range of motion for the actuator as well as improve the hysteresis of the device.

ACKNOWLEDGEMENT

The project was also supported by the National Science Foundation (ECCS 2029077) and a seed fund from Temple University

REFERENCES

[1] Mosadegh, B., Polygerinos, P., Keplinger, C., Wennstedt, S., Shepherd, R. F., Gupta, U., … Whitesides, G. M. (2014). "Soft Robotics: Pneumatic Networks for Soft Robotics that Actuate Rapidly" (Adv. Funct. Mater. 15/2014). Advanced Functional Materials, 24(15), 2109–2109. doi: 10.1002/adfm.201470092

[2] Holz, B., Riccardi, L., Janocha, H., & Naso, D. (2012). "MSM Actuators: Design Rules and Control Strategies.", Advanced Engineering Materials, 14(8), 668–681. doi: 10.1002/adem.201200045

[3] Kim, Y., Yuk, H., Zhao, R., Chester, S. A., & Zhao, X. (2018). "Printing ferromagnetic domains for untethered fast-transforming soft materials." Nature, 558(7709), 274–279. doi: 10.1038/s41586-018-0185-0

[4] Alici, G. (2015). "Towards soft robotic devices for site-specific drug delivery.", Expert Review of Medical Devices, 12(6), 703–715. doi: 10.1586/17434440.2015.1091722

[5] Hwang, J., Kim, J.-Y., & Choi, H. (2020). "A review of magnetic actuation systems and magnetically actuated guidewire- and catheter-based microrobots for vascular interventions.", Intelligent Service Robotics, 13(1), 1–14. doi: 10.1007/s11370-020-00311-0

[6] Potekhina, & Wang. (2019). "Review of Electrothermal Actuators and Applications". *Actuators*, *8*(4), 69. doi: 10.3390/act8040069

[7] Brando, A., Mayumi, K., Yokoyama, H., and Ito, K. (2013), "Theory of volume phase transition of slide gel rings ", Reactive and Functional Polymers, 73: 904-910. doi:10.3390/polym8060217

[8] Wemyss-Holden, S.A., Berry, D.P., Robertson, G.S.M., Dennison, A.R., De La M Hall, P. and Maddern, G.J. (2002), "Electrolytic ablation as an adjunct to liver resection: Safety and efficacy in patients", ANZ Journal of Surgery, 72: 589-593. doi:10.1046/j.1445-2197.2002.02471.x

[9] Park et al., “A Wireless Chemical Sensing Scheme Using Ultrasonic Imaging of Silica-Particle-Embedded Hydrogels (Silicagel),” Sensors and Actuators B Chemical . 259, 2017

[10] Song et al., “A Wireless Chemical Sensor Featuring Iron Oxide Nanoparticle-Embedded Hydrogels,” Sensors and Actuators B: Chemical. 193: 925-930, 2014.

[11] N. A. Peppas, "Kinetics of smart hydrogels," *Reflexive Polymers and Hydrogels: Understanding and Designing Fast-responsive Polymeric Systems, CRC Press, Boca Raton, FL*, pp. 99–113, 2004.

[12] Du, K., Ding, J., Liu, Y., Wathuthanthri, I., & Choi, C.-H. (2017). "Stencil Lithography for Scalable Micro- and Nanomanufacturing.", Micromachines, 8(4), 131. doi: 10.3390/mi8040131

CONTACT

*Albert Kim, tel: +1-215-204-3222; albertkim@temple.edu